INTERNATIONAL JOURNAL OF CLIMATOLOGY
Int. J. Climatol. **25**: 1–16 (2005)
Published online in Wiley InterScience (www.interscience.wiley.com). DOI: 10.1002/joc.1087

SIGNALS OF ANTHROPOGENIC INFLUENCE ON EUROPEAN WARMING AS SEEN IN THE TREND PATTERNS OF DAILY TEMPERATURE VARIANCE

A. M. G. KLEIN TANK,* G. P. KÖNNEN and F. M. SELTEN
Royal Netherlands Meteorological Institute, De Bilt, The Netherlands

Received 19 April 2004
Revised 21 June 2004
Accepted 22 June 2004

ABSTRACT

Signals of anthropogenic warming over Europe are searched for in the spatial trend patterns for the variance and skewness (expressed by the 10th and 90th percentiles) of the distribution of daily mean temperature. Comparisons are made between these patterns in the station records of the European Climate Assessment dataset for the 1976–99 period, the patterns associated with natural variability in the observations (which were empirically derived from the observations in the 1946–75 period), and the patterns of future warming and natural variability as simulated by the National Center for Atmospheric Research Community Climate System Model in the Challenge ensemble experiment.

The results indicate that, on the basis of the patterns for the variance, a distinction can be made between temperature change due to natural variability and temperature change due to changes in external forcing. The observed variance trend patterns for the spring (March–May) and summer (June–August) warming 1976–99 are clearly different from the patterns for the change in variance associated with a warming due to natural variability in the observations. This led us to conclude that a change in an external forcing has to be invoked to explain the observed spring and summer warming. From the evaluation of the greenhouse and natural variability patterns in the climate model simulations, we infer that the observed spring and summer variance trend patterns contain imprints consistent with anthropogenic warming. The analysis of the variance trend patterns for the winter (December–February) season is inconclusive about identifying causes of the observed warming for that season. Unlike the other three seasons, the autumn (September–November) is for Europe a period of cooling in recent decades. The observed variance trend pattern for this season closely resembles the estimated pattern for the change in variance associated with a cooling due to natural variability, indicating that the observed autumn cooling can be ascribed to random weather variations in the period under consideration.

KEY WORDS: climate change; detection; attribution; daily climate extremes; European climate; anthropogenic causes; global warming

1. INTRODUCTION

Like for the world, higher future temperatures are expected for Europe as a result of anthropogenic climate change (Houghton *et al*., 1990, 1996, 2001). This prospect of significant human-induced warming has led to increasing interest in the detection of anthropogenic signals in observational records of the past. Whether such signals are actually seen in the temperature records of the last century depends on the spatial scale considered. At the global scale, Houghton *et al*. (2001) conclude that: 'most of the warming observed over the last 50 years is attributable to human activities'. At the continental scale, the attribution of the observed warming to anthropogenic influence is not (yet) firmly settled due to the larger natural variability in the records. However, positive results of such analyses are starting to be reported. Recently, Stott (2003) detected the warming effects of increasing greenhouse gas concentrations in six separate land areas of the Earth, including Europe. Zwiers and Zhang (2003) were able to identify the greenhouse gas and sulphate aerosol-induced signal in the observed annual mean near-surface temperatures of the past 50 years over North America

* Correspondence to: A. M. G. Klein Tank, Royal Netherlands Meteorological Institute, PO Box 201, 3730 AE De Bilt, The Netherlands; e-mail: albert.klein.tank@knmi.nl

and Eurasia. Other regional detection studies are in progress (International Ad Hoc Detection and Attribution Group, 2004).

Anthropogenic signals have not yet been positively detected at all in series of extreme events (International Ad Hoc Detection and Attribution Group, 2004), despite their obvious relevance for society. The fact that extremes are, by definition, rare and observational series relatively short reduces the detectability of statistically significant trends in extremes, let alone trends that are induced by human activities. Other facts that hamper the detection of human-induced changes in extremes are the lack of high-resolution datasets, data inhomogeneities and uncertainties in climate model predictions of changes in extremes.

In our previous study of daily temperature extremes in Europe (Klein Tank and Können, 2003), we were able to detect significant changes in moderate, also called 'soft', extremes with average return periods of 5–60 days. In that study, we used indices recommended by the joint working group on climate change detection of the World Meteorological Organization-Commission for Climatology (WMO-CCL) and the Research programme on climate variability and predictability (CLIVAR; Peterson *et al.*, 2001). For the 1976–99 episode of strong and persistent warming over Europe, we found differences in the warming of the cold and warm tails of the distributions of daily maximum temperature and daily minimum temperature. Studying some of the same indices in observations and climate models, Kiktev *et al.* (2003) provide evidence that human-induced forcing has recently played an important role in extreme climate. However, they did not consider indices for both the cold and the warm tail of the daily temperature distributions.

The objective of the present study is to investigate whether the differential warming of the tails of the daily temperature distributions contains a possible clue for the attribution of the changes to anthropogenic influence. This is done by investigating whether the characteristics of the European warming of the recent past are different from the characteristics associated with natural temperature variability as derived from previous decades and whether similar differences are seen in climate model simulations of current and future climate. Daily mean temperature is investigated. Although a series of daily mean temperature is roughly equal to the average of maximum and minimum temperature, this does not imply that the daily distributions of these quantities show similar behaviour. The differential warming of the cold and warm tails of the daily mean temperature distribution studied here may be different from the differential warming found in Klein Tank and Können (2003) for maximum and minimum temperature.

As before, we focus on 'soft' temperature extremes at a daily resolution. Soft extremes are defined as extremes with return periods of 5–60 days, which means that the annual number of events is sufficiently large to allow for meaningful trend analysis in a $\sim$50 year time series (Klein Tank and Können, 2003: equation (3)). The soft extremes in the present study are the 10th and 90th temperature percentiles rather than the corresponding day-count indices used in Klein Tank and Können (2003). This choice is motivated by the fact that percentiles are less sensitive to inhomogeneities in the series than day-count indices and by the fact that the use of percentiles avoids potential problems with the lower (zero) bound in day-count indices. The 10th and 90th temperature percentiles form the basis for two carefully defined distribution measures that summarize variance and skewness. For these two distribution measures and for the mean, the trend patterns in the observations for the 1976–99 period are compared with the patterns associated with a warming due to natural variability. The latter were derived empirically from the earlier 1946–75 period, this being an episode with little temperature change over Europe. Also for the variance, skewness and mean, the trend patterns in the climate model simulations of future warming are compared with the patterns associated with a warming due to natural variability in the climate model.

We argue that, if the characteristics of the strong warming of the recent past are anomalous compared with natural variability, the trend patterns in one or more of the distribution measures may contain an imprint of anthropogenic warming. If the same measures in the climate model also show significant differences between the trend patterns for future warming under enhanced atmospheric greenhouse gas concentrations and the patterns associated with natural variability, then the trend pattern for that particular measure is sensitive for anthropogenic warming indeed. Formal detection techniques, like pattern-correlation methods (e.g. Santer *et al.*, 1995) or optimal detection methods (e.g. Hasselman, 1979), require realistic climate model estimates of natural variability and model fingerprints of forced climate change signals. These techniques have meanwhile evolved in sophisticated space–time and space–frequency detection studies (e.g. Stott *et al.*, 2001). Our approach is different, in that we empirically separate regional climate characteristics that are likely to be associated with a warming due to natural variability from characteristics that are likely to be associated with anthropogenic change. We do this separation on the basis of the patterns of a few simple measures for the daily temperature distribution, rather than on the basis of model estimates of (combined) greenhouse gas/aerosol patterns.

In our analysis, a seasonal breakdown of the trend patterns is advisable, because the specific atmospheric circulations that govern the temperatures (including extremes) over Europe have a different effect in each season. In large parts of Europe, circulations with airflow from the continent (snow-covered in winter; hot in summer) lead to cold extremes in winter and warm extremes in summer. Likewise, airflow from the Atlantic Ocean is associated with warm extremes in winter and cold extremes in summer. Thus, a change in the frequency of a particular atmospheric circulation pattern has different effects on the trend patterns of temperature extremes in each season (Luterbacher *et al*., 2004; Schaeffer *et al*., 2004). The measures selected for the daily temperature distribution are suitable to reveal such differences.

Section 2 describes the observational series from the daily station dataset of the European Climate Assessment (ECA; Klein Tank *et al*., 2002a) and the climate model data from the Challenge experiment (Selten *et al*., in press). Section 3 details the measures that are used to summarize the daily temperature distribution. The procedure for estimation of trend patterns in the observations and model simulations and the procedure for partitioning changes due to natural variability and trends due to changes in non-natural external forcing are outlined in Section 4. Section 5 presents the results, which are discussed in Section 6.

2. DATA

A selection of daily series of temperature observations at meteorological stations in Europe was taken from the ECA dataset (Klein Tank *et al*., 2002b). As in Klein Tank and Können (2003), the selection criteria were based on series completeness, adequate data coverage of Europe and homogeneity ranking (Wijngaard *et al*., 2003). The present study employs the ECA dataset version October 2003 for the period 1946–99, in which the selection yields a total of 185 station series (Figure 1(a)) for which the daily mean temperature series met the criteria.

Climate model data are from ensemble integrations with the Community Climate System Model (CSM) version 1.4 of the National Center for Atmospheric Research (NCAR), which is a fully coupled global climate model. The ensembles were produced in the so-called Challenge experiment (Selten *et al*., in press), in which the CSM has been used to produce 62 simulations of the Earth's climate for the period 1940–2080, each starting from a slightly perturbed initial atmospheric state. The initial state of the other parts of the climate system was not perturbed. Between 1940 and 2000 the radiative forcings are according to historical estimates of atmospheric composition, solar irradiance and sulphate and volcanic aerosols. From 2000 until the year

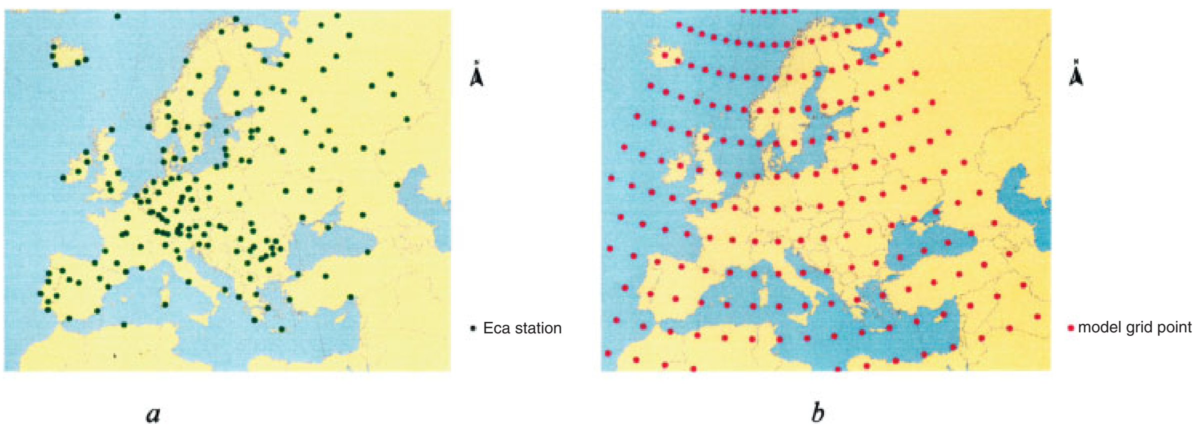

Figure 1. ECA stations (a) and Challenge model grid points (b) used in this study

2080 the radiative forcing change is calculated according to the business-as-usual emission scenario of NCAR, which is similar to the SRES A1b scenario of the Intergovernmental Panel on Climate Change (Houghton *et al*., 2001). From the Challenge simulations, we use the daily mean near-surface air temperature data from all 62 members for grid points in a European window of the model (Figure 1(b)). Considered is the period 1946–99, which corresponds with the ECA observations, as well as the period 2046–75 for future warming.

3. MEASURES TO SUMMARIZE THE DISTRIBUTION OF DAILY MEAN TEMPERATURE

The distribution of daily mean temperature is summarized by three descriptive measures: the mean MEA, and the variance VAR and skewness SKEW as expressed by the quantiles P10, P50 and P90, being the 10th percentile, the median and the 90th percentile respectively. The measures VAR and SKEW give information about the shape of the distribution and primarily relate to the soft extremes in the tails of the distribution. The choice to express VAR and SKEW by the 10th and 90th percentiles rather than more extreme quantiles is motivated by the possibility to detect trends in extremes given the length of the record (see in Klein Tank and Können (2003: equation (3)). The variance VAR and the skewness SKEW are defined as follows:

$$\mathrm{VAR} = \frac{\mathrm{P90} - \mathrm{P10}}{2} \tag{1}$$

$$\mathrm{SKEW} = \frac{\mathrm{P90} - \mathrm{P50}}{\mathrm{P50} - \mathrm{P10}} \tag{2}$$

In this definition, VAR and SKEW are discrete expressions of the full statistical definitions of standard deviation and skewness. They are special cases of the sample L-scale and sample L-skewness parameters in Hosking (1990), which are known to be more robust than conventional moments to outliers in the data (Hosking, 1990). The units for MEA and VAR are centigrade; SKEW is dimensionless. In the definition of SKEW in Equation (2), the median P50 instead of the mean MEA was used. The reason is that, contrary to the mean, the median is not affected by a change occurring in one tail of the distribution only. For daily temperature distributions, the median is usually close to the mean. SKEW in Equation (2) ranges from $[0, \infty]$, with $\mathrm{SKEW} = 1$ corresponding to no skewness.

For the study periods, the annual and seasonal values of the three distribution measures MEA, VAR and SKEW were calculated for each observation station and model grid point as follows. First, the percentile values P10, P50 and P90 were calculated for 5-day windows centred on each calendar day to account for the mean annual cycle. This yields a total sample size of $5N$ days, with N the length of the study period in years. The calendar day percentile values were then averaged over the year and the seasons: winter (December, January, February; DJF), spring (March, April, May; MAM), summer (June, July, August; JJA) and autumn (September, October, November; SON). No smoothing was applied (cf. Klein Tank and Können, 2003). The 62 members of the climate model were treated as a single distribution, yielding sample sizes of $62 \times 5N$ days for each calendar day. Jenkinson's empirical ranking formula (Folland and Anderson, 2002) was used to calculate the percentile values P10, P50 and P90. This formula gives satisfactory results for the (soft) extremes considered here (Folland and Anderson, 2002).

Table I shows the climatological values of MEA, VAR, SKEW, P10, P50 and P90 based on the standard normal period 1961–90 for five selected stations in different areas of Europe. The values for the grid points in the climate model nearest to the five stations are also given. The Europe-averages in Table I are calculated from the average values of MEA, P10, P50 and P90 over all ECA stations.

The values in Table I are illustrative for the climate conditions over Europe with regard to extremes. They show that Europe-average values of VAR are almost twice as high in winter than summer, with intermediate values in the transition seasons. This feature is in accordance with the fact that winter temperature variability is usually higher than summer temperature variability. The values of VAR vary greatly across Europe: the Russian station has the highest values of VAR (up to 9.4 °C for winter), which is typical for a continental climate. In the Mediterranean region, VAR is much smaller and its annual course is also small. The lowest

Table I. Climatological values of the measures that summarize the distribution of daily mean temperature over the 1961–90 baseline period for five stations from different areas of Europe. The values for the nearest grid points in the NCAR climate model (Challenge ensemble experiment) are given in parentheses. The Europe-average represents a mean over all ECA stations. MEA is the mean temperature; VAR and SKEW are the variance and skewness as expressed by the temperature percentiles P10, P50 and P90. SKEW = 1 implies no skewness. All units are centigrade, except for SKEW, which has no dimension

	Reykjavik (Iceland)	Elatma (Russia)	De Bilt (Netherlands)	Salamanca (Spain)	Larissa (Greece)	Europe-average
Annual						
MEA	4.4 (4.9)	4.3 (2.1)	9.4 (8.8)	11.7 (14.4)	15.7 (14.7)	8.2
VAR	3.9 (4.6)	6.3 (8.3)	4.2 (3.3)	4.0 (3.1)	3.7 (3.5)	4.8
SKEW	0.8 (0.7)	0.8 (0.7)	1.0 (0.7)	1.0 (0.9)	0.9 (0.8)	0.9
P10	0.4 (−0.1)	−2.2 (−7.0)	5.2 (5.2)	7.7 (11.3)	11.9 (11.1)	3.2
P50	4.6 (5.3)	4.7 (3.0)	9.3 (9.2)	11.6 (14.5)	15.8 (14.9)	8.3
P90	8.1 (9.1)	10.3 (9.6)	13.7 (11.8)	15.6 (17.4)	19.4 (18.0)	12.9
Winter (DJF)						
MEA	−0.1 (1.1)	−9.5 (−13.4)	2.6 (4.4)	4.4 (10.3)	6.1 (7.2)	−1.0
VAR	5.4 (6.5)	9.4 (14.1)	5.5 (4.6)	4.2 (2.7)	4.4 (4.4)	6.5
SKEW	0.8 (0.6)	0.7 (0.7)	0.7 (0.5)	1.1 (0.7)	0.9 (0.7)	0.8
P10	−5.8 (−6.1)	−19.5 (−28.8)	−3.3 (−0.8)	0.3 (7.4)	1.7 (2.4)	−7.8
P50	0.4 (2.0)	−8.5 (−11.9)	3.1 (5.4)	4.3 (10.6)	6.2 (7.7)	−0.5
P90	5.0 (6.9)	−0.7 (−0.7)	7.8 (8.3)	8.7 (12.8)	10.4 (11.3)	5.1
Spring (MAM)						
MEA	3.3 (2.7)	4.9 (1.2)	8.4 (5.9)	10.1 (11.7)	14.4 (12.6)	7.4
VAR	4.2 (5.2)	6.2 (8.0)	4.2 (3.6)	4.3 (2.9)	3.9 (3.6)	4.9
SKEW	0.8 (0.7)	0.9 (0.6)	1.1 (0.7)	1.1 (1.1)	1.0 (1.0)	1.0
P10	−1.2 (−2.9)	−1.4 (−7.7)	4.4 (2.1)	5.9 (8.8)	10.5 (9.0)	2.4
P50	3.6 (3.2)	5.3 (2.4)	8.3 (6.3)	10.0 (11.6)	14.4 (12.6)	7.4
P90	7.2 (7.5)	11.0 (8.2)	12.7 (9.3)	14.5 (14.6)	18.2 (16.2)	12.3
Summer (JJA)						
MEA	10.0 (9.3)	17.3 (15.6)	16.2 (14.4)	19.7 (19.5)	26.0 (22.5)	17.3
VAR	1.9 (2.8)	4.7 (4.4)	3.7 (2.0)	3.6 (3.5)	3.3 (2.6)	3.9
SKEW	1.0 (1.0)	1.0 (0.9)	1.7 (1.1)	1.0 (1.1)	1.0 (1.1)	1.1
P10	8.0 (6.5)	12.7 (11.1)	12.9 (12.4)	16.0 (16.1)	22.7 (19.9)	13.5
P50	10.0 (9.4)	17.3 (15.8)	15.7 (14.3)	19.8 (19.5)	26.0 (22.4)	17.2
P90	11.9 (12.1)	22.0 (19.8)	20.3 (16.4)	23.3 (23.1)	29.3 (25.1)	21.3
Autumn (SON)						
MEA	4.3 (6.3)	4.3 (4.7)	10.2 (10.3)	12.3 (16.0)	16.3 (16.3)	8.9
VAR	4.1 (3.9)	5.5 (6.9)	3.9 (3.2)	4.1 (3.3)	3.9 (3.3)	4.6
SKEW	0.9 (0.8)	0.8 (0.7)	0.9 (0.7)	0.9 (0.9)	0.8 (0.7)	0.9
P10	0.1 (2.3)	−1.4 (−2.7)	6.2 (6.8)	8.1 (12.7)	12.2 (12.7)	4.2
P50	4.4 (6.5)	4.7 (5.3)	10.2 (10.6)	12.4 (16.2)	16.5 (16.7)	9.1
P90	8.4 (10.1)	9.6 (11.1)	14.0 (13.2)	16.2 (19.2)	20.0 (19.4)	13.4

value of VAR (1.9 °C) is observed in the summer for the station in Iceland, whose (maritime) climate is very equable compared with the other stations. The measure SKEW reveals other peculiarities. For the autumn and winter season, all stations have values smaller than unity, except Salamanca (Spain) in winter. SKEW values smaller than unity imply that (P50 − P10) > (P90 − P50), i.e. the cold tail (P50 − P10) is heavier than the warm tail (P90 − P50). This indicates that cold outbreaks occur more frequently or are more severe than warm outbreaks in Europe during autumn and winter. For the spring season, values both smaller than unity and larger than unity are found for SKEW. For the summer season, all stations show SKEW = 1 (no skewness), except De Bilt. The high value of 1.7 for SKEW at this station illustrates that relatively severe warm summer spells occur in the otherwise mild summer climate near the west coast of Europe, where airflow from the nearby sea dominates.

Table I also shows that the climate model simulates the annual mean temperature at the five selected stations reasonably well, although the warm biases for MEA in winter and the cold biases for MEA in summer indicate that the annual cycle in the model is generally too weak. The exception here is the Russian station, for which the model simulates winter temperatures that are too low. The low winter temperatures are accompanied by values of P10 that are far too low, implying that very cold winter days are abundantly simulated by the model. Incorrect simulation of the amount of snow cover by the model may contribute to the temperature bias during winter. Daily temperature variability expressed by VAR is too high for the Icelandic and Russian stations and too low for the Dutch and Spanish stations. The values of SKEW are reasonably well reproduced by the model, with the anomalous summer value of 1.7 at station De Bilt a marked exception.

4. TREND ESTIMATION AND ATTRIBUTION METHODOLOGY

Robust trend analysis was used to determine the trends in the three distribution measures MEA, VAR and SKEW. This method compares the values in the first half of a period with the values in the second half by means of a t-test. The analysis was performed for all ECA stations and for all model grid points shown in Figure 1.

For the observations, the trend patterns in the three distribution measures were determined for the period 1976–99, this being an episode of pronounced warming in Europe (on average ~0.7 °C/decade). To establish the patterns of change associated with a warming due to natural variability, the 1946–75 period, being an episode of little temperature change, was split into a set of cold and a set of warm years. The cold set consists of all years with Europe-average temperature below the 1946–75 median and the warm set consists of all years with Europe-average temperature above the 1946–75 median. This splitting procedure is illustrated in Figure 2. The same procedure was applied for each of the four seasons. The differences in Europe-average temperature between the cold and warm sets are 0.6 °C for the year, and 2.1 °C, 1.1 °C, 0.6 °C and 0.8 °C for the winter, spring, summer and autumn respectively. Then, the patterns for the change in MEA, VAR and SKEW associated with a warming due to natural variability were calculated as the difference between the two sets for each station. They can be interpreted as resulting from a reordering of years that would have produced an artificial trend representative for an accumulation of overall warming due to natural variability. For instance, if a Europe-average warming due to natural variability of 0.4 °C is found for a 20 year period, then it is caused by an unequal distribution of warm and cold years in that episode. In that case, the detected Europe-average trend is 0.2 °C/decade, and the patterns of ΔMEA, ΔVAR and ΔSKEW should be the same as those obtained by the splitting procedure. Note that, within the chosen framework, the splitting procedure introduces an upper bound to the Europe-average temperature rise by natural variability of 0.6 °C for the year. The estimates for the patterns associated with a warming due to natural variability (being the difference between the cold and warm set of years) will not change when shorter (or longer) periods are considered. The robustness of the ΔVAR patterns associated with a warming due to natural variability as derived from the 1946–75 period was tested by calculating the patterns separately for the sub-periods 1946–60 and 1961–75.

The splitting procedure assumes that natural variability primarily acts at short time scales ($\leq$1 year). The effect of natural variability at longer time scales was verified to be sufficiently small by considering a cold and warm set of temperature averages in two and three consecutive years instead of 1 year. This choice did not change the conclusions. Surface air-pressure fields from the National Centers for Environmental Prediction–NCAR reanalysis data (Kalnay *et al*., 1996) confirm that the splitting procedure is able to represent the small-scale spatial structures that are typically associated with natural temperature variability over Europe (not shown).

For the climate model, the trend patterns for anthropogenic climate change were calculated as the difference between the Challenge simulated values for the 1946–75 period (first half) and those for the 2046–75 period

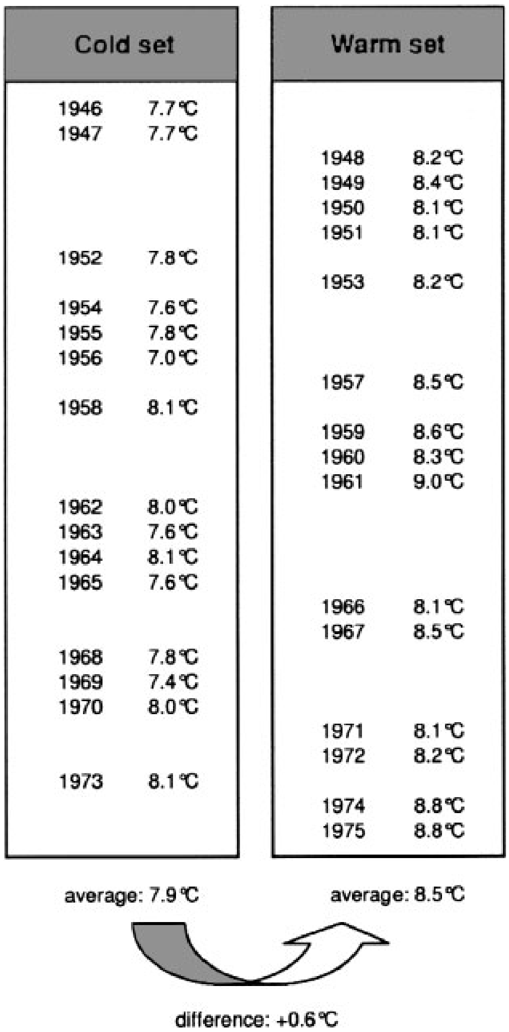

Figure 2. Cold and warm sets of years distinguished on the basis of the Europe-average temperatures in the 1946–75 period. The patterns for the change in mean temperature ΔMEA, variance ΔVAR and skewness ΔSKEW associated with a warming due to natural variability are determined empirically by subtracting the patterns of MEA, VAR and SKEW for the cold set from the patterns of MEA, VAR and SKEW for the warm set. If a warming in a certain time interval arises from random weather variations, then the observed trend patterns of MEA, VAR and SKEW should correspond with the patterns of ΔMEA, ΔVAR and ΔSKEW estimated by the splitting procedure described above

(second half). The Europe-average anthropogenic warming in the model is ~0.2 °C/decade. Given the fact that the 62 ensemble members were treated as a single distribution, the characteristic signal of greenhouse forcing is well determined in this way, because the major part of natural variability cancels out. The patterns associated with a warming due to natural variability in the model were calculated from the 1946–75 simulations, following the same splitting procedure as with the observations and treating the 62 members of the climate model as a single distribution. The differences in Europe-average temperature between the cold set and the warm set in the model are 0.3 °C for the year, and 0.6 °C, 0.4 °C, 0.1 °C and 0.3 °C for the winter, spring, summer and autumn seasons respectively. The patterns associated with a warming due to natural variability in the model obtained by the splitting procedure are in good agreement with the simulated warming patterns for the member exhibiting the largest Europe-average temperature increase in the 1946–75 period (correlation >0.6). This supports the robustness of our splitting procedure.

Next, systematic comparisons were made for each of the three distribution measures between the trend patterns in the observations for the 1976–99 period and the estimated patterns associated with a warming due to natural variability in the observations. The same was done between the trend patterns in the climate model simulations of future warming and the estimated natural variability patterns in the climate model. The spatial resemblance of the patterns was examined by visual inspection and using fixed pattern-correlation techniques (Hegerl *et al*., 1996). To guide the interpretation of the comparisons, the following conceptual relation is applied for the trend patterns in the 1976–99 period:

$$\Psi_s \text{ (observed)} = a\Psi_s \text{ (forced)} + b\Psi_s \text{ (natural)} \quad (3)$$

with Ψ_s the characteristic trend pattern for MEA and VAR in season s, a the trend portion due to changes in non-natural external forcing and b the trend portion due to warming/cooling by natural variability. Equation (3) also holds in first order for SKEW, but since the SKEW trend pattern is generally more noisy than the VAR trend pattern, SKEW is only used to double check the results obtained with VAR.

If the patterns of trends and the patterns associated with natural variability for a distribution measure are different both in the observations and in the climate model, then the observed 1976–99 patterns possibly contain an imprint of anthropogenic warming over Europe. The following assumptions are made, which are partly validated with ECA and Challenge data:

- the changes associated with a warming due to natural variability have a unique signature in the spatial patterns of ΔVAR and ΔSKEW;
- this unique signature of the changes associated with a warming due to natural variability can be obtained by the splitting procedure applied to a period of little overall temperature change, such as 1946–75.

5. RESULTS

5.1. Mean temperature trends 1976–99

Figure 3 shows the station trends for mean temperature MEA observations in the 1976–99 period for the year and each of the 3-month seasons. Warming trends dominate, with, on average, the strongest warming in winter. Apart from a north–south gradient, there is a weaker gradient from the ocean to the continent. As a result, the overall highest temperature rises are found over central and northeastern Europe and the lowest temperature rises over the Mediterranean and Iceland. The spatial gradients in winter (Figure 3(b)) are much stronger than those in summer (Figure 3(d)). In winter, the strongest warming (up to about 3 °C/decade) is observed over northern Europe, whereas southern Europe shows little warming, or even cooling over Greece and Turkey. In summer, the warming pattern is much flatter, with trends roughly between 0.5 and 1.5 °C/decade throughout Europe. An intermediate trend pattern is found in spring (Figure 3(c)), with cooling rather than warming over Iceland.

The autumn season (Figure 3(e)) is a prominent exception to the overall temperature rise. It shows significant cooling up to about 1 °C/decade over a large area of the continent. This result is in good agreement with the autumn cooling over parts of Europe found in the gridded temperature dataset from Jones *et al*. (2001; see Houghton *et al*. (2001: 117, figure 2.10d)).

5.2. Imprints of anthropogenic warming

The climate model simulations of future warming indicate that anthropogenic forcing leads to warming in every season (not shown). Clearly, this fact alone does not imply that the winter, spring and summer trend patterns of mean temperature MEA in Figure 3 contain imprints of anthropogenic warming. Our estimates of the patterns for the change in MEA associated with a warming due to natural variability (as derived from the observations in the 1946–75 period) indicate that, on the basis of natural variability alone, the possibility

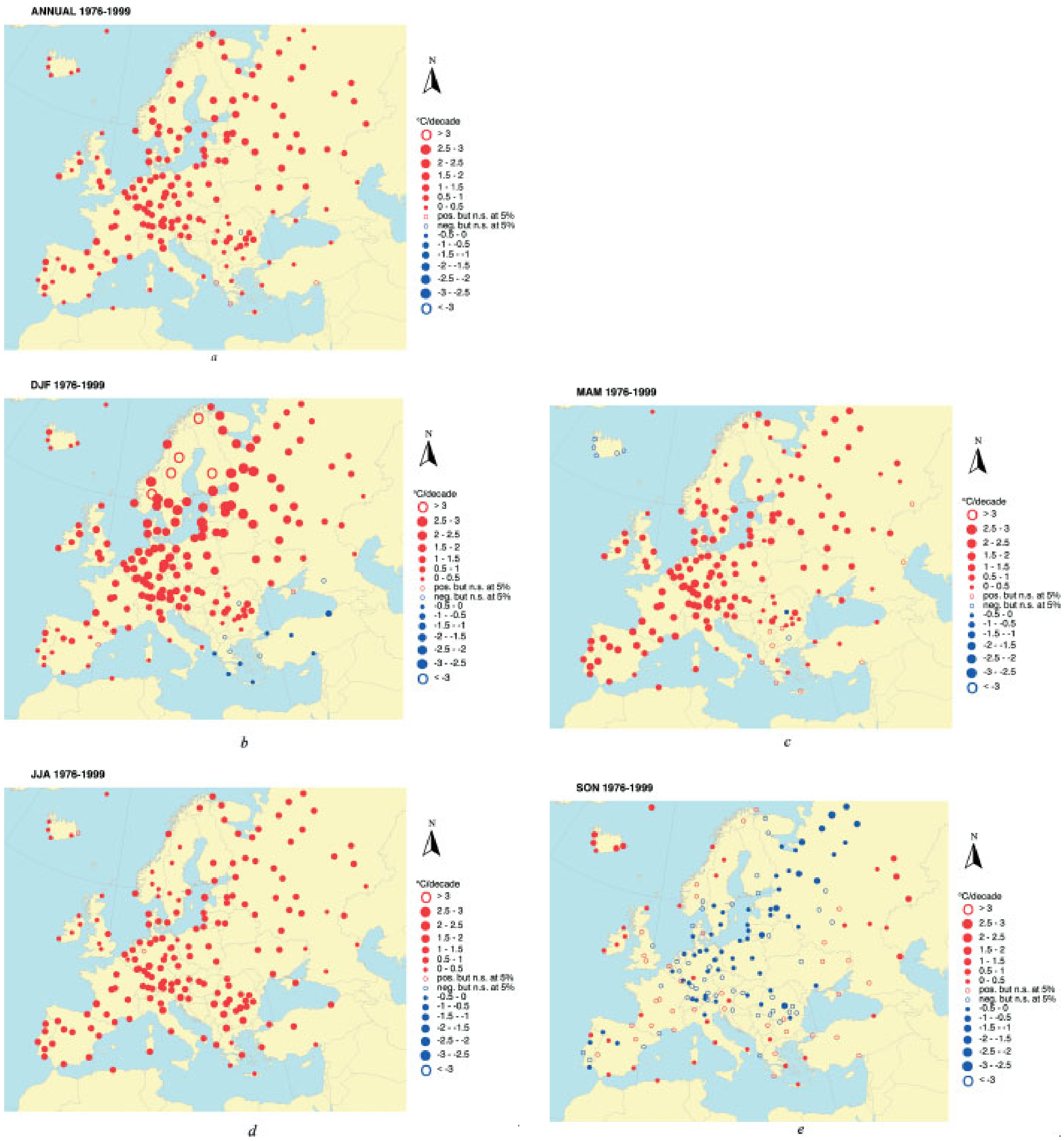

Figure 3. Trends per decade for mean temperature MEA observations in the 1976–99 period for (a) the year, (b) winter DJF, (c) spring MAM, (d) summer JJA and (e) autumn SON. The dots are scaled according to the magnitude of the trend. Colour coding is applied: red corresponds to warming trends, blue to cooling trends

exists of a warming without changes in external forcing that has a similar pattern to the observed temperature rise between 1976 and 1999. Table II shows that the spatial correlation coefficients between the observed trend patterns and the patterns associated with natural variability are significant at the 5% level for all seasons. The values range between 0.23 for spring and 0.71 for winter. Therefore, partitioning of the observed temperature change in either forced warming or natural variability on the basis of MEA is inconclusive, and most so for winter.

The situation is different, however, for the measure of variation VAR and, to a lesser extent, the measure of skewness SKEW. A plausible distinction between the two causes of warming (forced and natural) can be

Table II. Spatial correlation coefficients between the observed trend patterns 1976–99 and the estimated patterns associated with natural variability for the observations (top) and the same for the climate model simulations of future warming and natural variability in the model (bottom). Values significant at the 5% level (two-tailed) are set in bold

	Winter (DJF)	Spring (MAM)	Summer (JJA)	Autumn (SON)
Observations				
MEA	**0.71**	**0.23**	**0.55**	**−0.55**
VAR	**0.18**	0.10	0.04	**−0.45**
SKEW	**0.49**	0.07	−0.05	−0.03
Climate model				
MEA	**0.78**	**0.67**	**0.38**	**0.76**
VAR	**−0.41**	**−0.16**	**0.21**	**0.15**
SKEW	**−0.18**	**0.14**	**0.30**	**0.46**

made in several seasons on the basis of a comparison of the trend and natural variability patterns of these distribution measures.

For the autumn season, Figure 4 shows that the observed cooling is accompanied by an increase in temperature variance (Figure 4(a)). This VAR trend pattern is in good agreement with the ΔVAR pattern associated with natural variability (Figure 4(b)), if the signs are reversed. The spatial correlation coefficient between the observed pattern and that of natural variability is −0.45 (Table II). Note that the negative sign is due to the fact that the pattern associated with natural variability was derived for a warming situation, rather than for a cooling situation; the same pattern with a reversed sign would have been derived for a cooling situation. In the climate model, the VAR trend pattern for the future warming scenario (Figure 4(c)) differs from the ΔVAR pattern associated with natural variability in the model (Figure 4(d); correlation 0.15). This leads us to the conclusion that the observed autumn cooling in the 1976–99 period is primarily associated with natural variability.

For the spring season, the VAR trend pattern indicates that the observed warming cannot be explained by natural variability, because the pattern in the observations between 1976 and 1999 in Figure 5(a) is clearly different from the pattern associated with a warming due to natural variability in Figure 5(b) (correlation 0.10). The climate model also indicates differences between the simulations of future warming (Figure 5(c)) and natural variability in the model (Figure 5(d); correlation −0.16). Therefore, it is likely that forced warming dominates over natural variability.

The situation for summer resembles that for spring. The observed summer VAR trend pattern in Figure 6(a) is different from the pattern associated with a warming due to natural variability in Figure 6(b) (correlation 0.04), and a similar difference is also found for the climate model simulations (Figure 6(c) and (d); correlation 0.21).

For the winter season, attempts to partition the observed temperature change into either forced warming or natural variability are less successful. The winter VAR trend patterns (not shown) give no conclusive answer at all about a dominant warming cause. Figure 7 presents the corresponding trend patterns for skewness SKEW. The figure and the correlation coefficients in Table II also show that the intrinsically noisier SKEW patterns give no indication of significant differences between the trend patterns and the patterns associated with natural variability.

Table III qualitatively summarizes the results of the comparison between the trend and variability patterns, identifying possible imprints of anthropogenic warming in the spring VAR trend pattern and the summer VAR trend pattern.

Finally, Figure 8 shows the patterns for ΔVAR associated with a warming due to natural variability as estimated from the sub-periods 1946–60 (Figure 8(a)) and 1961–75 (Figure 8(b)) for the spring (MAM) season. A comparison with the corresponding pattern estimated from the full 1946–75 period in Figure 5(b) (repeated in Figure 8(c) for convenience) shows that the splitting procedure leads to robust estimates of the patterns associated with natural variability. The correlation coefficients between the 1946–60 and 1946–75

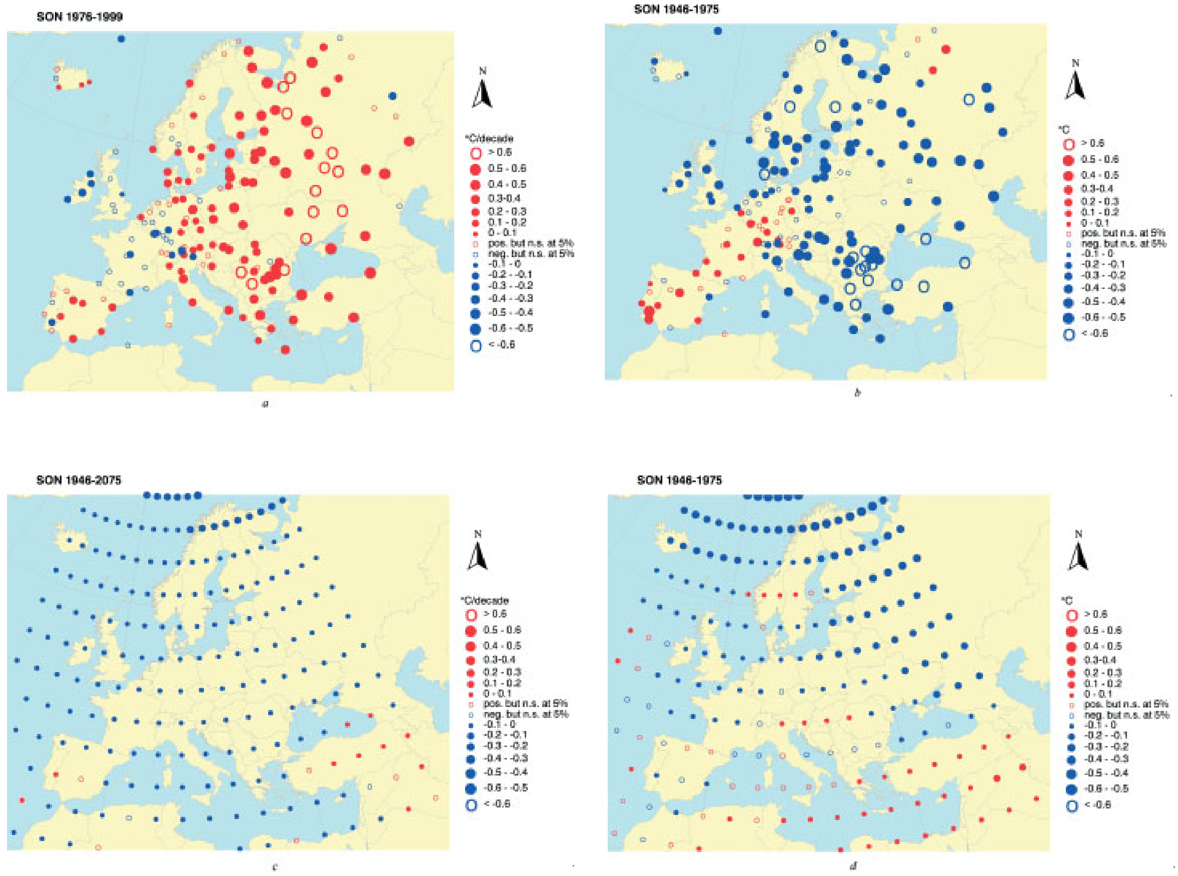

Figure 4. Autumn SON trends per decade for variance VAR in the observations for the 1976–99 period (a) and in the climate model simulations of future warming (c) together with the estimated ΔVAR patterns associated with a warming due to natural variability in the observations (b) and in the climate model (d). The latter were based on the 1946–75 period; for details see the text and Figure 2. The dots are as described in Figure 3

patterns and between the 1961–75 and 1946–75 patterns are 0.44 and 0.70 respectively. The correlation coefficients between these patterns for the other seasons (not shown) are ∼0.6.

6. DISCUSSION

On the basis of three measures for the distribution of daily mean temperature, we found that some of the seasonal patterns representing characteristics of European warming in the 1976–99 period are distinct from the estimated patterns that result from natural temperature variability. In particular, the observed spring (MAM) and summer (JJA) trend patterns for the measure of variance VAR are distinct from the estimated patterns for the change in VAR associated with a warming due to natural variability. Since the trend patterns in the climate model simulations of future warming for this measure are different from the estimated patterns associated with natural variability in the climate model as well, we conclude that the 1976–99 spring VAR and summer VAR trend patterns may contain imprints consistent with anthropogenic warming. For the warming in the winter season, no clear distinction could be made between forced warming and natural warming. The higher temperature variability in the European winter is a possible explanation. For the autumn season, the results indicate that natural temperature variability is the most likely cause for the cooling observed over a large part of the continent, as the autumn pattern of the trends in VAR is very similar to the estimated pattern for

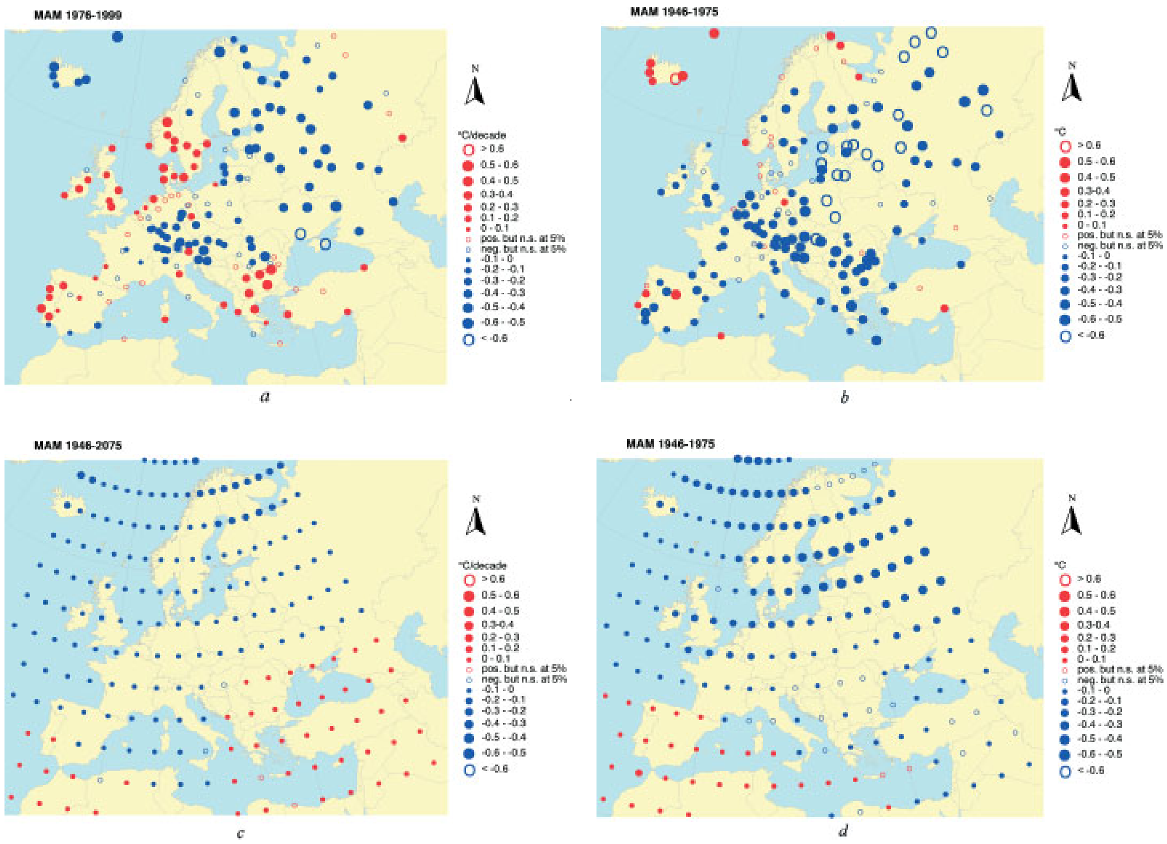

Figure 5. As Figure 4, but for spring MAM

the change in VAR associated with a cooling due to natural variability, whereas the climate model suggests clear differences between these patterns as a result of anthropogenic forcing. Consequently, for the autumn season, factor b in Equation (3) for the trend portion due to natural variability is negative and dominant with respect to factor a for the trend portion due to non-natural externally forced warming. In our view, this finding illustrates the power of our method.

A potential weakness of our method is that we obtained an estimate for the typical patterns associated with natural variability by artificially ranking the series of years (or seasons) in the 1946–75 period according to ascending Europe-average temperature. This simple method applied to a relatively short period can only partially account for the contribution from multidecadal natural climate variability to the recent warming. We feel that this is acceptable, because the method is primarily intended to search for a possible imprint of anthropogenic warming in the measures that reflect the warming characteristics of the tails of the daily temperature distribution in the 1976–99 period. No formal attribution to anthropogenic influence is sought for. Our method relies on the existence of a unique signature of the changes associated with a warming due to natural variability in the spatial patterns of ΔVAR and ΔSKEW that can be estimated from a period with little overall temperature change, such as 1946–75. This is supported by the fact that the estimated patterns do not change markedly when they are based on the sub-periods 1946–60 or 1961–75, instead of 1946–75. Our method is further supported by the fact that the estimated patterns associated with natural variability in the climate model resemble the trend patterns for the ensemble member in Challenge that has the greatest Europe-average warming in the 1946–75 period due to natural variability in the climate model simulations.

Formal climate change detection/attribution studies are required to determine whether the VAR trend patterns identified for 1976–99 can indeed be attributed to anthropogenic influence. Such studies involve direct comparisons between the observations and the climate model data. A preliminary analysis of the

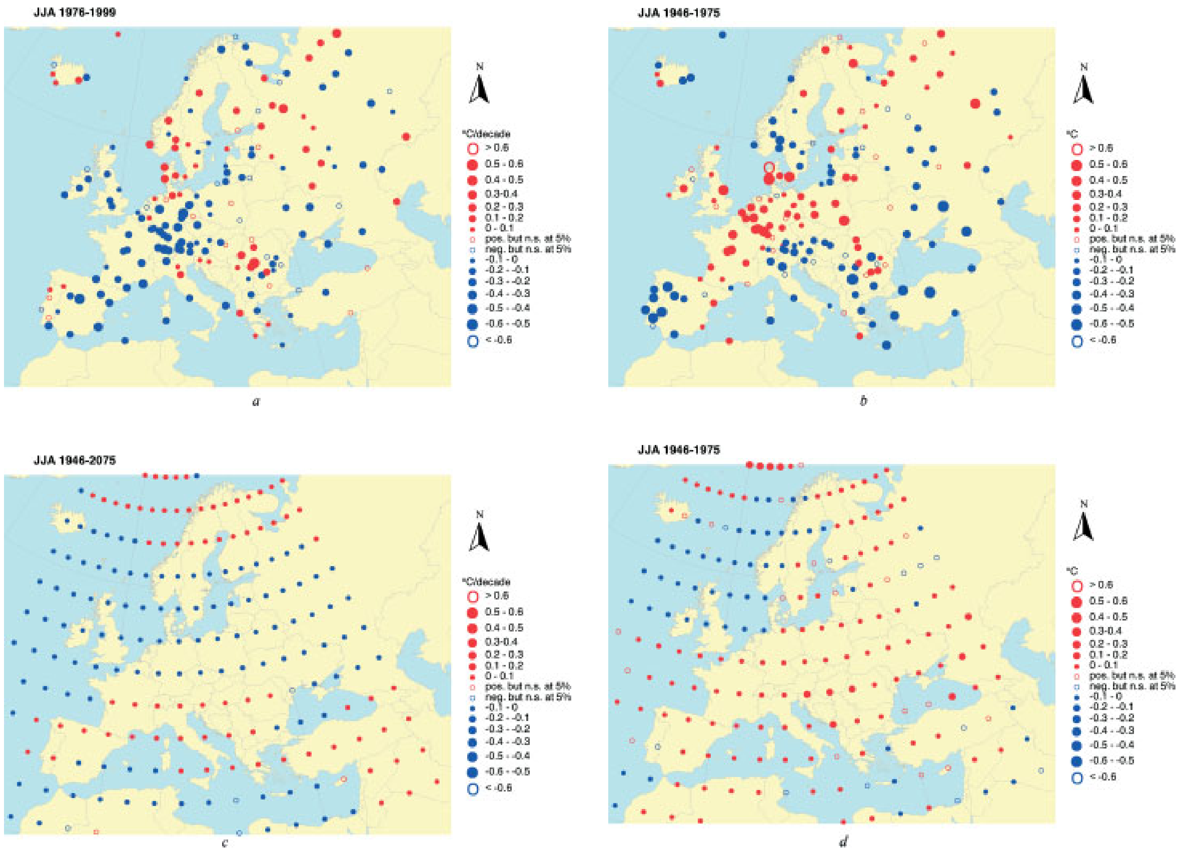

Figure 6. As Figure 4, but for summer JJA

climate model data from the Challenge experiment suggests that the model that was used is not suitable for such formal detection/attribution. The variance and skewness trend patterns observed in the ECA station data are not satisfactorily reproduced by the (older version of the) CSM used in Challenge.

The advantage of the Challenge data for our study is that the trend patterns for the future warming resulting from anthropogenic forcing are well defined, because the major part of natural variability cancels out in the ensemble mean derived from 62 climate model simulations. The Challenge data could be further analysed to find out in how many ensemble members the imprints of anthropogenic warming can be detected using our method and how this number grows when the analysis period is extended beyond 1999 into the future. The 62 Challenge simulations underline that for an adequate representation of the characteristics of the daily temperature distribution in Europe by more state-of-the-art general circulation models (GCMs) it is essential that these GCMs account for the natural variability that exists under the same external forcings (Selten *et al.*, in press). Natural variability means that the trend patterns for MEA, VAR and SKEW for a single simulation (such as an individual member in Challenge) do not need to be in close agreement with those in the ECA observations, even in a perfect model. Natural variability also makes it difficult to give an adequate interpretation of the differences in the climatological values of the distribution measures we found in Table I between the Challenge ensemble mean and the ECA data.

The measures we selected to represent the distribution of daily mean temperature proved to be able to separate in a plausible way the characteristics of forced warming from the characteristics of natural variability as derived from the 1946–75 period. Dominant causes for the temperature change between 1976 and 1999 could be identified for all seasons except winter. Although VAR and SKEW are based on the same series of daily mean temperatures, they are independent quantities with respect to MEA. Clearly, VAR is less noisy

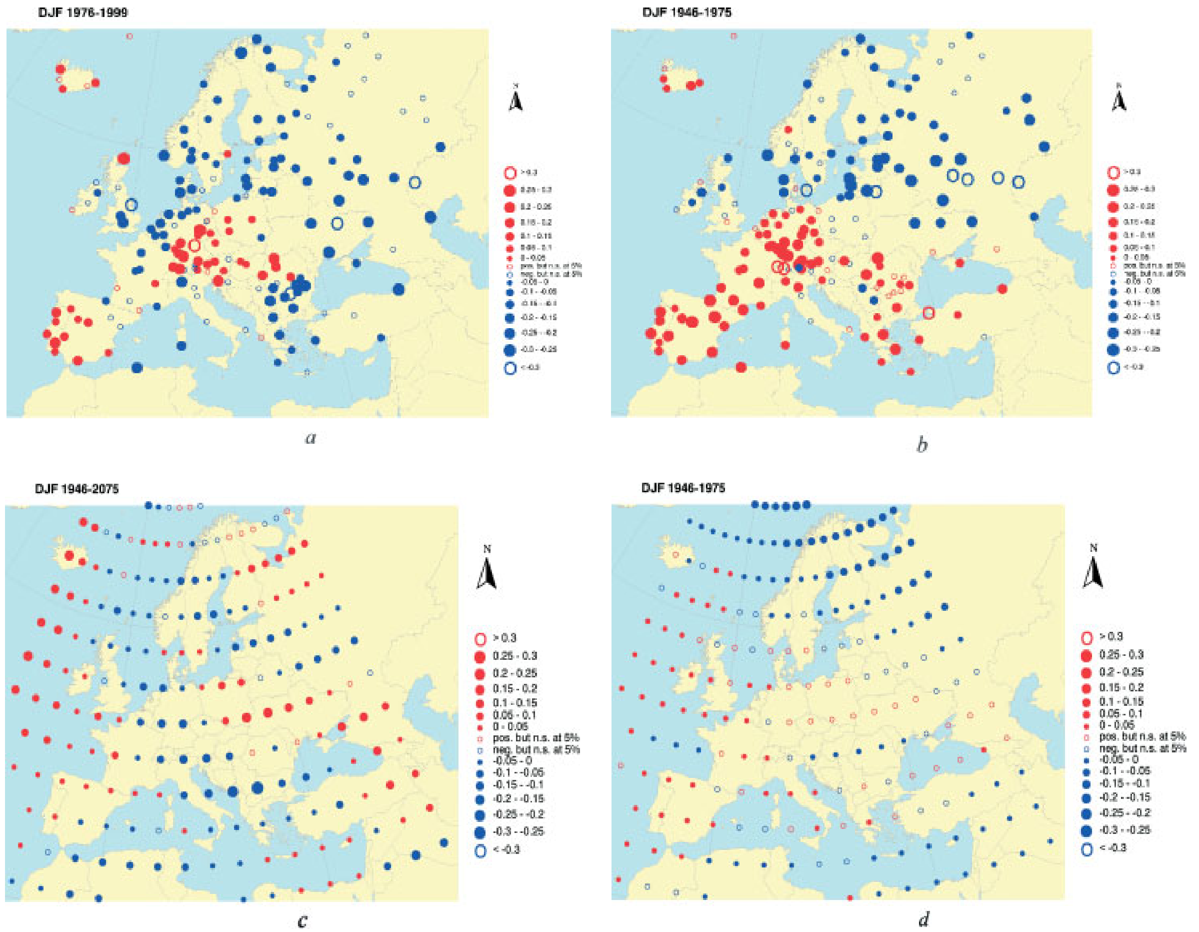

Figure 7. As Figure 4, but for skewness SKEW in winter DJF

Table III. Qualitative judgement of the results of the pattern comparison between observed trends and estimates of the changes associated with natural variability. Categories are: forced, indicating that an imprint consistent with anthropogenic warming is seen; natural variability, indicating that natural variability dominates; inconclusive, indicating that partitioning is not successful

	Winter (DJF)	Spring (MAM)	Summer (JJA)	Autumn (SON)
MEA	Inconclusive	Inconclusive	Inconclusive	Inconclusive
VAR	Inconclusive	Forced	Forced	Natural variability
SKEW	Inconclusive	Forced	Forced	Natural variability

and, therefore, generally more suitable than SKEW. Among the possible reasons for the fact that the clearest signals of anthropogenic warming are found in the VAR trend patterns for spring are the amplifying effects of changes in the onset of spring and the amplifying effects of changes in snow cover. The fact that signals of anthropogenic warming are also found in the summer VAR trend patterns may be related to the soil moisture feedback associated with changes in summer precipitation (see Schär *et al.* (2004)).

Future climate change detection/attribution studies may profit from the results of our explorative analysis when choosing the measures that are prime candidates for the fingerprints of forced climate change signals. First studies in this direction (Hegerl *et al.*, 2004) already suggest that changes in soft temperature extremes

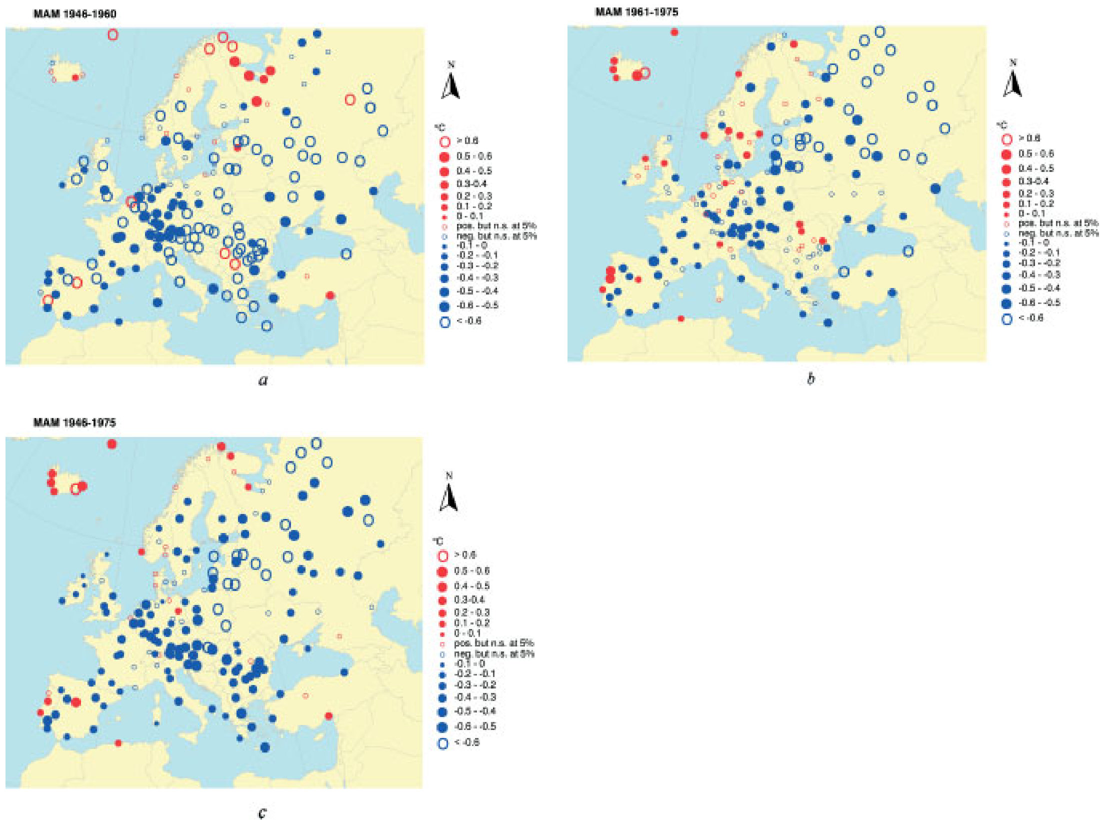

Figure 8. Spring MAM patterns for ΔVAR associated with a warming due to natural variability as derived from the observations in the 1946–60 period (a) and the 1961–75 period (b), compared with the corresponding pattern derived from the observations in the full 1946–75 period (c, repeated from Figure 5(b)). The good agreement between the patterns for the three different base periods is illustrative for the robustness of the splitting procedure (see Figure 2)

should be nearly as detectable as changes in mean temperature. The trend patterns of the distribution measures that we identified in the present study may be among the sensitive fingerprints for the early detection of anthropogenic change in climate extremes.

ACKNOWLEDGEMENTS

We thank P.D. Jones and a second (anonymous) reviewer for their valuable comments on the original manuscript. We also thank the participants in the European Climate Assessment (ECA) project (supported by the Network of European Meteorological Services EUMETNET). ECA data are available at www.knmi.nl/samenw/eca. Challenge Website: www.knmi.nl/onderzk/CKO/Challenge_live/Engels.

REFERENCES

Folland C, Anderson C. 2002. Estimating changing extremes using empirical ranking methods. *Journal of Climate* **15**: 2954–2960.
Hasselman K. 1979. On the signal-to-noise problem in atmospheric response studies. In *Meteorology of Tropical Oceans*, Shaw DB (ed.). Royal Meteorological Society: 251–259.
Hegerl GC, von Storch H, Hasselmann K, Santer BD, Cubasch U, Jones PD. 1996. Detecting greenhouse-gas-induced climate change with an optimal fingerprint method. *Journal of Climate* **9**: 2281–2306.
Hegerl GC, Zwiers FW, Stott PA, Kharin VV. 2004. Detectability of anthropogenic changes in annual temperature and precipitation extremes. *Journal of Climate* **17**: 3683–3700.
Hosking JRM. 1990. L-moments: analysis and estimation of distributions using linear combinations of order statistics. *Journal of the Royal Statistical Society* **52**: 105–124.

Houghton JT, Jenkins GJ, Ephraums JJ (eds). 1990. *Climate Change: The IPCC Scientific Assessment*. Cambridge University Press: Cambridge, UK.
Houghton JT, Meira Filho LG, Callander BA, Harris N, Kattenberg A, Maskell K (eds). 1996. *Climate Change 1995: The Science of Climate Change*. Cambridge University Press: Cambridge, UK.
Houghton JT, Ding Y, Griggs DJ, Noguer M, van der Linden PJ, Dai X, Maskell K, Johnson CA (eds). 2001. *Climate Change 2001: The Scientific Basis*. Cambridge University Press: Cambridge, UK.
International Ad Hoc Detection and Attribution Group. 2004. Detecting and attributing external influences on the climate system: a review of recent advances. *Journal of Climate* submitted for publication.
Jones PD, Osborn TJ, Briffa KR, Folland CK, Horton EB, Alexander LV, Parker DE, Rayner NA. 2001. Adjusting for sampling density in grid box land and ocean surface temperature time series. *Journal of Geophysical Research* **106**: 3371–3380.
Kalnay E, Kanamitsu M, Kistler R, Collins W, Deaven D, Gandin L, Iredell M, Saha S, White G, Woollen J, Zhu Y, Chelliah M, Ebisuzaki W, Higgins W, Janowiak J, Mo KC, Ropelewski C, Wang J, Leetmaa A, Reynolds R, Jenne R, Joseph D. 1996. The NCEP/NCAR 40-year reanalysis project. *Bulletin of the American Meteorological Society* **77**: 437–471.
Kiktev D, Sexton DMH, Alexander L, Folland CK. 2003. Comparison of modelled and observed trends in indices of daily climate extremes. *Journal of Climate* **16**: 3560–3571.
Klein Tank A, Wijngaard J, van Engelen A. 2002a. Climate of Europe; assessment of observed daily temperature and precipitation extremes. KNMI, De Bilt, The Netherlands. eca.knmi.nl [Accessed April 2004].
Klein Tank AMG, Wijngaard JB, Können GP, Böhm R, Demarée G, Gocheva A, Mileta M, Pashiardis S, Hejkrlik L, Kern-Hansen C, Heino R, Bessemoulin P, Müller-Westermeier G, Tzanakou M, Szalai S, Pálsdóttir T, Fitzgerald D, Rubin S, Capaldo M, Maugeri M, Leitass A, Bukantis A, Aberfeld R, van Engelen AFV, Forland E, Mietus M, Coelho F, Mares C, Razuvaev V, Nieplova E, Cegnar T, Antonio López J, Dahlström B, Moberg A, Kirchhofer W, Ceylan A, Pachaliuk O, Alexander LV, Petrovic P. 2002b. Daily dataset of 20th-century surface air temperature and precipitation series for the European Climate Assessment. *International Journal of Climatology* **22**: 1441–1453.
Klein Tank AMG, Können GP. 2003. Trends in indices of daily temperature and precipitation extremes in Europe, 1946–1999. *Journal of Climate* **16**: 3665–3680.
Luterbacher J, Dietrich D, Xoplaki E, Grosjean M, Wanner H. 2004. European seasonal and annual temperature variability, trends, and extremes since 1500. *Science* **303**: 1499–1503.
Peterson TC, Folland C, Gruza G, Hogg W, Mokssit A, Plummer N. 2001. Report on the activities of the Working Group on Climate Change Detection and Related Rapporteurs 1998–2001. Report WCDMP-47, WMO-TD 1071, World Meteorological Organization, Geneva, Switzerland.
Santer BD, Taylor KE, Penner JE, Wigley TML, Cubasch U, Jones PD. 1995. Towards the detection and attribution of an anthropogenic effect on climate. *Climate Dynamics* **12**: 77–100.
Schaeffer M, Selten FM, Opsteegh JD. 2004. Shifts of means are not a proxy for changes in extreme winter temperatures in climate projections. *Climate Dynamics* submitted for publication.
Schär C, Vidale PL, Lüthi D, Frei C, Häberli C, Liniger MA, Appenzeller C. 2004. The role of increasing temperature variability in European summer heatwaves. *Nature* **427**: 332–336.
Selten FM, Branstator G, Dijkstra HA, Kliphuis M. In press. Tropical origins for recent and future Northern Hemisphere climate change. *Geophysical Research Letters*.
Stott PA, Tett SFB, Jones GS, Allen MR, Ingram WJ, Mitchell JFB. 2001. Attribution of twentieth century temperature change to natural and anthropogenic causes. *Climate Dynamics* **17**: 1–21.
Stott PA. 2003. Attribution of regional-scale temperature changes to anthropogenic and natural causes. *Geophysical Research Letters* **30**: 1728, Doi: 10.1029/2003GL017324.
Wijngaard JB, Klein Tank AMG, Können GP. 2003. Homogeneity of 20th century European daily temperature and precipitation series. *International Journal of Climatology* **23**: 679–692.
Zwiers FW, Zhang X. 2003. Toward regional-scale climate change detection. *Journal of Climate* **16**: 793–797.

